

1 **Supporting Information**

2

3 **Competitive growth kinetics of coexisting hydrogen bubbles**  
4 **on Ni electrodes: role of bubble nucleation density**

5 Weikang Yang<sup>a,\*</sup>, Dongxu Gu<sup>b</sup>, Xin Liu<sup>a</sup>, Qiangmin Luo<sup>a</sup>

6 *<sup>a</sup> School of Chemistry and Chemical Engineering, Chongqing University,*  
7 *Chongqing 400044, PR China.*

8 *<sup>b</sup> Institute of Intelligent Innovation, Henan Academy of Sciences, Zhengzhou,*  
9 *Henan, 451162, P. R. China.*

10 \*Corresponding author. *E-mail: wkyang@stu.cqu.edu.cn; Phone: +86 18725737346.*

11

12

13

14

15

16

17

18

19

20

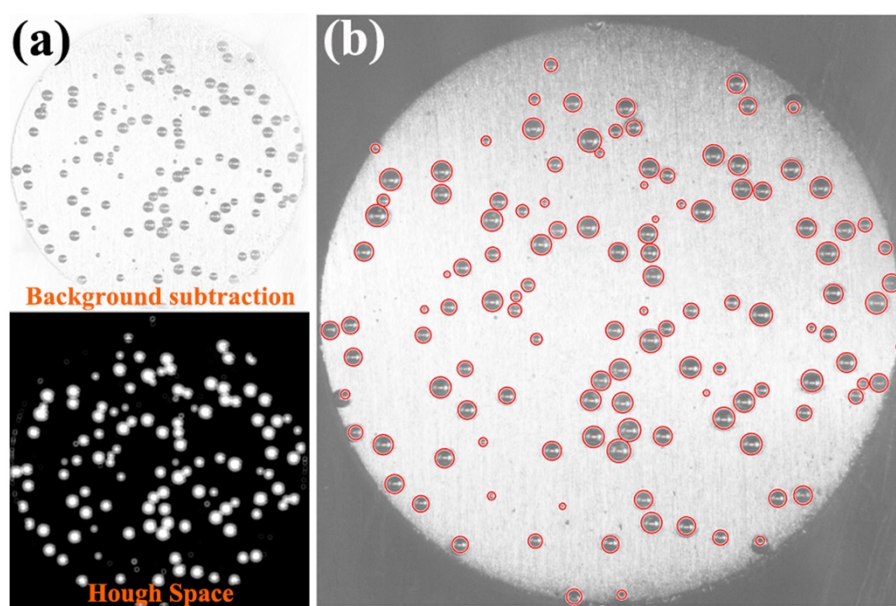
21

22

23

## 24 1. Image analysis program

25 The image analysis program was developed based on the image processing  
26 module of MATLAB (R 2022b). As shown in Figure S1a, the acquired images were  
27 pre-processed to obtain the best recognition effect. For the identification of multiple  
28 bubbles in the image, the Hough algorithm were employed in our program, and the  
29 recognition results were shown in Figure S1b.



30  
31 **Figure S1.** (a) The image after pre-processing, (b) The recognition results of multiple bubbles.

## 32 33 2. Micro-bubble adhesion test device constructed with the AFM

34 Figure S2 illustrated the basic principle of measuring adhesion  
35 between bubble and electrode by using Atomic Force Microscope (AFM).  
36 During the test, the cantilever approached the substrate under the control  
37 and reached the critical value of triggering, the cantilever was far away  
38 from the substrate. The force on the cantilever tip was determined by the  
39 bending degree of the cantilever and the spring constant of the cantilever.

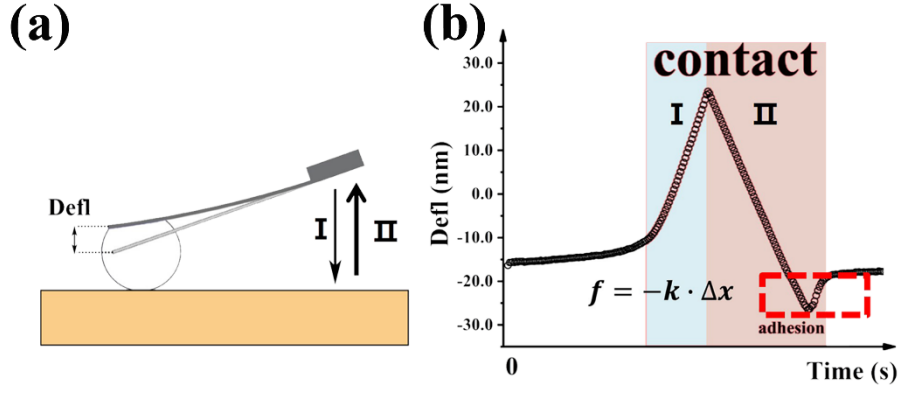


**Figure S2.** The basic principle of measuring adhesion between bubble and electrode by using AFM.

In order to obtain the quantitative adhesion force, the inverse optical lever sensitivity (invOLS) was calibrated by performing a single force curve on a silicon substrate as a hard non-deformable substrate. As shown in Figure S3a, the invOLS in our experimental was 101.06 nm/V, which is magnification of the electrical signal caused by the bending degree of the cantilever. The spring constant of the cantilever (HQ-13-Au-1<sup>st</sup>-2) used in our experimental was confirmed to 0.133 nN/nm by the thermal method provided from Hutter and Bechhoefer (Figure S3b).

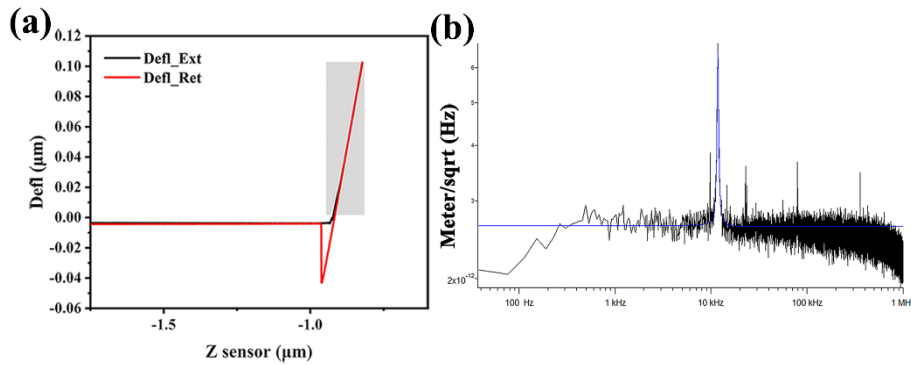
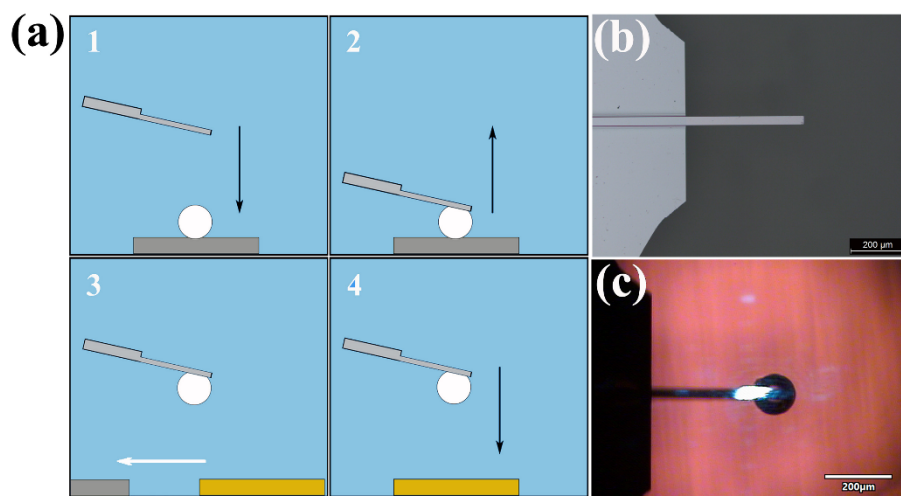


**Figure S3.** (a) The inverse optical lever sensitivity (invOLS), (b) The thermal data of the cantilever (HQ-13-Au-1<sup>st</sup>-2).

55

56 To assemble the bubble probe, the hydrophobic cantilever was  
57 observed through the light microscope of MFP-3D and moved onto the  
58 appropriate bubble. By controlling the cantilever down, the bubble was  
59 picked up from the silicon surface and moved towards the target samples  
60 (Figure S4).



61  
62 **Figure S4.** (a) The way to assemble the adhesion test device, (b) The microscopic image of the  
63 cantilever (HQ-13-Au-1<sup>st</sup>-2), (c) The bubble probe in light microscope of MFP-3D.

64

65 Considering that the resistance of underwater movement could not be  
66 ignored, the adhesion force of the bubble and the Ni electrode was tested  
67 by setting different approaching velocity of the cantilever, and the results  
68 were shown in Figure S5. As the approaching velocity decreased, the  
69 adhesion force decreased until the velocity reach 400 nm/s, which was  
70 considered as the bubble adhesion force excluding the influence of the  
71 approaching velocity, and the results were listed in Table S1.

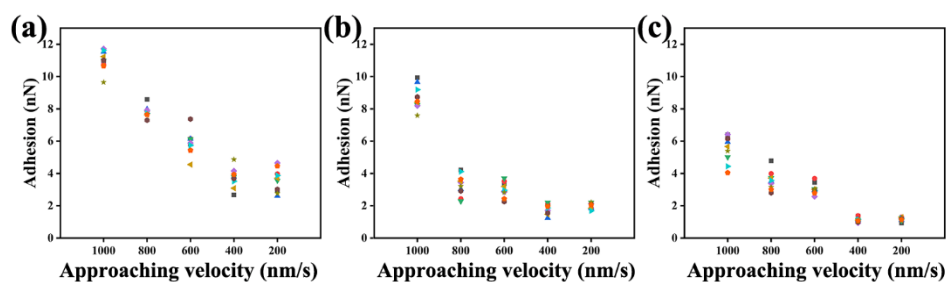


**Figure S5.** (a) The way to assemble the adhesion test device, (b) The microscopic image of the cantilever (HQ-13-Au-1<sup>st</sup>-2), (c) The bubble probe in light microscope of MFP-3D.

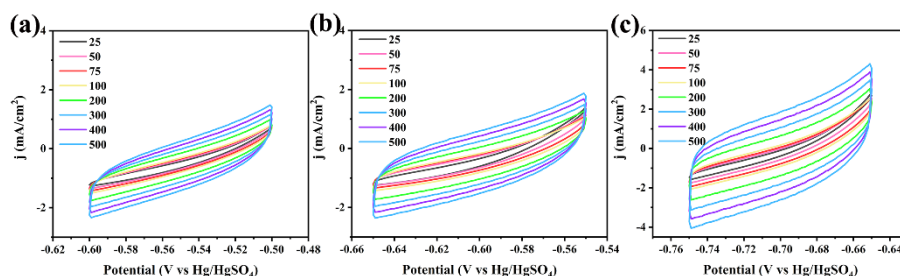
**Table S1. The adhesion force of the bubble and the Ni electrode (nN)**

Approaching velocity	1000 (nm/s)	800 (nm/s)	600 (nm/s)	400 (nm/s)	200 (nm/s)
<i>HR-surface</i>	5.56±1.52	3.56±1.22	3.05±0.64	1.12±0.25	1.16±0.22
<i>MR-surface</i>	8.71±1.22	3.28±0.99	3.01±0.75	1.82±0.58	2.01±0.32
<i>LR-surface</i>	11.00±1.35	7.82±0.77	5.87±1.50	3.74±1.13	3.56±1.09

### 3. The cyclic voltammetry results of the electrodes

As shown in Figure S3, the cyclic voltammetry near the open-circuit voltage, with a voltage range of 50 mV, was employed in each Ni electrode to obtain its double-layer capacitance at various scanning speeds. In this potential region, the electrode surface remains in the non-faradaic zone, where the measured current corresponds to the charging/discharging current of the electric double layer (EDL). The magnitude of the EDL charging/discharging current depends on the potential scan rate. The slope obtained from the linear fitting of current density (geometric area) versus different scan rates represents the EDL capacitance of the electrode surface. Conventionally, the roughness factor are normalized by the EDL capacitance of an ideal smooth metal surface (60  $\mu\text{F}/\text{cm}^2$ ) to quantify the increased EDL capacitance

89 caused by surface roughness, which correlates with the real surface area of electrode.  
 90 In this study, a simplified approach was adopted, where normalization was performed  
 91 using only the LR (roughness surface).



92  
 93 **Figure S6.** (a) The cyclic voltammetry of the HR-surface electrode under different scanning  
 94 speeds, (b) The cyclic voltammetry of the MR-surface electrode under different scanning speeds,  
 95 (c) The cyclic voltammetry of the LR-surface electrode under different scanning speeds.